ORIGINAL PAPER

An environmental and economic evaluation of solar photovoltaic thermal dryer

A. Gupta[1] · B. Das[1,2] · A. Biswas[1] · J. D. Mondol[2]

Abstract

The photovoltaic thermal (PVT)-based solar dryer is advantageous in terms of energy-saving ability, efficiency, self-sufficient design, and ability to work without any additional electrical energy requirement. However, there is a requirement for a comprehensive analysis of the energy, exergy, and environ-economic parameters for developing an efficient and sustainable PVT solar dryer. In this study, a PVT-based indirect mode solar dryer with forced convection has been fabricated and investigated in the environmental conditions of North-East India (Silchar latitude of 24.83°). Experiments have been performed to compare the drying characteristics of tomatoes with quality analysis under the open sun and solar drying conditions. A new mathematical drying model is proposed to predict the drying characteristics of tomatoes under both modes of drying. The average PVT dryer efficiency is 34.98%, higher than some of the published works of indirect mode solar dryers conducted under similar experimental conditions. The calculated values of drying effectiveness, collector efficiency factor, coefficient of performance, and heat utilization factor are 1.12–1.58, 0.011–0.029, 0.71, and 0.29, respectively. Furthermore, CO_2 emission, CO_2 mitigation and carbon credit earned parameters are evaluated for 10, 20, and 30 years of system life.

Graphical abstract
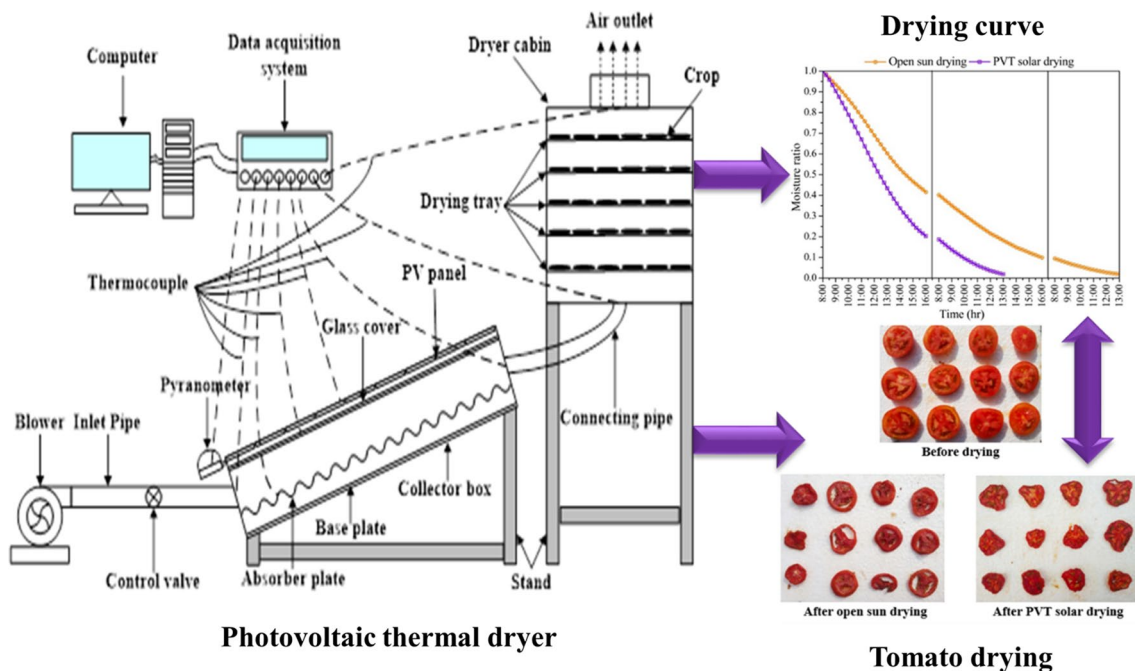
Photovoltaic thermal dryer

Tomato drying

List of symbols

A_m	Module area (m^2)
c_{pwf}	Working fluid specific heat (J/kg K)
E_i	Embodied energy (W)
E_{el}	Electrical energy (W)
$I(s)$	Solar radiation (W/m^2)
L_s	System life (Y)
m_e	Mass of evaporation (kg/s)
MC_d	Moisture content on dry basis (d.b.)
MC_w	Moisture content on wet basis (w.b.)
Q_{av}	Total energy available on PVTAC surface (W)
Q_e	Heat required to evaporate the sample moisture (W)
Q_g	Heat generated by PVTAC (W)
Q_{ov}	Overall energy generated by PVTAC (W)
$Q_{PVTAC,ex,in}$	Exergy input to PVTAC (W)
$Q_{PVTAC,ex,loss}$	Exergy loss from PVTAC (W)
$Q_{PVTAC,ex,ov}$	Overall exergy obtained from PVTAC (W)
$Q_{PVTAC,ex,th}$	Thermal exergy obtained from PVTAC (W)
T_a	Ambient air temperature (°C)
T_{co}	Collector outlet air temperature (°C)
T_{ci}	Collector inlet air temperature (°C)
T_{dco}	Dryer cabin outlet air temperature (°C)
T_{dci}	Dryer cabin inlet air temperature (°C)
T_{sc}	Solar cell temperature (°C)

Greek letter

η_{ov}	Overall efficiency of PVTAC (%)
η_{PVTAC}	Instantaneous efficiency of PVTAC (%)
$\eta_{PVTAC,ex}$	Exergy efficiency of PVTAC (%)
$\eta_{ov,ex}$	Overall exergy efficiency of PVTAC (%)
η_{PVTD}	PVT dryer efficiency (%)
η_{sc}	Solar cell efficiency (%)
γ_{dco}	Relative humidity at dryer outlet (%)
γ_{dci}	Relative humidity at dryer inlet (%)

Introduction

Solar energy is a promising source of energy to reduce dependence on non-renewable energy sources. Solar energy systems are the need for society, and they contribute to society by fulfilling the energy demands and mitigating carbon emissions. Solar energy can be converted into thermal and electrical energy (Kumar et al. 2015) in a single system using a photovoltaic thermal collector (PVTC), which is an alluring adaptation in the field of solar energy (Joshi and Dhoble 2018). The PVT systems have been widely adopted

in numerous fields to improve the overall energy output (Lamnatou and Chemisana 2017).

Drying with the open sun is utilized indiscriminately in many developing countries as a conventional open sun drying process (Singh et al. 2017). However, the possibility of crop spoilage increases in the open sun drying (OSD) process. This can be overcome by adopting the solar drying process. Various solar dryers, namely mixed mode (Andharia et al. 2020), indirect mode (Goud et al. 2019), direct mode (Dutta et al. 2020), greenhouse solar dryer (Chauhan et al. 2018a), PCM-based solar dryer (Lakshmi et al. 2018), solar dryer with heat storage (Vijayan et al. 2020), and PVT-based solar greenhouse dryer (Tiwari et al. 2016), have been investigated by different researchers. Among these solar drying systems, PVT-based solar dryers have enormous potential as these systems have a faster drying rate, higher energy output, and better temperature control, and provide better quality products. Previous studies showed that the permissible temperature range for the drying of different crops could be achieved by varying the packing area of the PV module (Jha et al. 2020a), air mass flow rate (Tiwari et al. 2018), and absorber design (Jha et al. 2019).

The drying performance of the PVT-based solar dryer developed by various researchers was investigated to determine the suitability of the solar drying system for practical applications. Samimi-Akhijahani and Arabhosseini (2018) proposed a PV-operated solar dryer with sun tracking to dry tomato slices. The drying time was shortened from 36.60 to 16.60% by using a sun tracker in the solar drying system. The selection of the PVT collector is one of the significantly essential criteria for developing the PVT solar dryer. Kong et al. (2020) performed solar dryers integrated with PVT air collectors for turnips drying. The system's average thermal and electrical efficiency was calculated as 46.80% and 5.70%, respectively, for amorphous silicon-type PVT collector, and 40.70% and 6.80%, respectively, for polysilicon-type PVT collector. Dorouzi et al. (2018) investigated the drying performance of tomatoes by changing drying temperature and relative humidity range of air in indirect mode solar dryer combined with PV panel. This study obtained 27.00% less drying time by changing relative humidity from 28.00 to 18.00% and temperature from 60 to 70 °C. Daghigh et al. (2019) dried tarkhineh in evacuated tube and PVT collector mode solar drying. Results indicated that the dryer efficiency was found to be 28.20% in evacuated tube solar dryer and 13.70% in PVT solar dryer mode.

The drying mode also affects the performance of the solar drying system. The performance was compared in different drying modes. Chauhan and Kumar (2018) compared PV integrated solar dryer performance in the open sun, passive

mode, and active mode. More accurate statistical parameter results of drying kinetics were achieved by Prakash and Kumar model (Singh and Kumar 2018) under passive mode with 41.00% less drying time than OSD mode. Cesar et al. (2020) compared the solar dryer performance in the mixed mode and indirect mode for tomato drying. The collector efficiency, dryer efficiency, and drying time for the mixed mode and indirect mode of drying were 55.45%, 52.30%, and 18 h, and 10.66%, 8.80%, and 27 h, respectively. Wang et al. (2017) reported that the dryer thermal efficiency was calculated to be in the range of 30.9–33.8% for mango drying. The temperature ranges of 40 °C, 44 °C, 48 °C, and 52 °C were used for studying the drying kinetics with the decreased drying time achieved at 52 °C, and better prediction for all temperature ranges was found in the Page model. Dejchanchaiwong et al. (2016) investigated rubber sheet drying performance with dryer efficiency of 13.30% and 15.40% in indirect mode and mixed-mode drying, respectively.

The research work done on energy, exergy, and techno-economic analysis for the solar dryer by various researchers is discussed in detail. Tiwari and Tiwari (2017a) studied PVT solar greenhouse dryers' energetic and exergetic performance with varying PVT air collectors from 1 to 5. As the number of PVT collectors increased, the energy and exergy efficiency decreased. Tiwari and Tiwari (2017b) developed a solar PVT greenhouse dryer to examine the performance of slurry heating. The total generation of energy was 1.65 kWh considering both thermal and electrical energy sources. Chauhan et al. (2018b) proposed a PV integrated greenhouse dryer using an innovative solar collector. It was found that the maximum energetic and exergetic efficiencies were 16.80% and 21.40%, and 18.40% and 24.50%, respectively, for with and without solar collector mode. Rabha et al. (2017) found an exergy efficiency of 47% and 63% for drying ginger and ghost chili pepper, respectively, for an indirect solar dryer. An indirect mode solar dryer energy and exergy efficiency for drying medicinal herb was measured as 26.10% and 0.81%, and 9.80% and 0.41%, respectively, for with and without sensible heat storage material by Bhardwaj et al. (2018). The exergy efficiency of a solar dryer operating in mixed mode for drying turmeric was found to be 49.12% by Karthikeyan and Murugavelh (2018). Hatami et al. (2020) found that the exergy flow was high at higher air velocity with lower irreversibility. The maximum exergy efficiency was obtained to be 22.00%, and there was no influence of the mass of the product on the exergy efficiency of the solar dryer. Tiwari and Tiwari (2016) developed a PVT-based solar greenhouse dryer and investigated the dryer performance for different sunshine hours on a monthly basis. The energy payback time, CO_2 emission, CO_2 mitigation, and carbon credit were 1.23 years, 170.08 kg/year, 81.75 tonnes, and 817.50$, respectively, over a 25 year lifetime.

The previous literature reveals that PVT-based solar dryers are finding major importance in solar drying applications due to their energy-saving ability and self-sustainable design, especially in rural areas with no grid connectivity. The solar dryers operated with indirect mode have better dryer performance. There is a possible up-gradation of indirect mode forced solar convection dryer into PVT-based solar dryer to work without any electrical requirements. The improved performance of drying can be achieved using a forced convection PVT solar dryer compared with an indirect mode solar dryer. Limited number of studies have been reported on PVT-based solar dryers of indirect mode (Kong et al. 2020; Daghigh et al. 2019), and mixed mode (Tiwari et al. 2016, 2017a,b). None of these studied drying kinetics of tomatoes in indirect mode forced convection PVT solar dryer with energy, exergy, and environ-economic parameters evaluation. The present work aims to improve the drying kinetics validation for tomato (Solanum Lycopersicum) drying using a new proposed drying model along with energy, exergy, and environ-economic analysis of an indirect mode forced convection PVT solar dryer.

The objectives of this study are as follows:

(a) To determine the thermal performance and energy parameters of the PVT-based indirect mode forced convection solar dryer.
(b) To indicate the useful energy achieved by the PVT system using exergy analysis for tomato slices drying.
(c) To develop a new drying model to predict the moisture values of tomato slices and improve the drying process compared to the available drying models.
(d) To perform environmental impact and economic analysis of the developed prototype unit.

Materials and methods

Description of the experimental setup

The designed photovoltaic thermal solar dryer (PVTSD) was mainly comprised of a photovoltaic thermal air collector (PVTAC), dryer cabin, blower, and connecting pipe. The tests were carried out in NIT Silchar, India (latitude of 24.83° N). The schematic diagram of the experimental setup is shown in Fig. 1a, and specification parameters are summarized in Table 1.

Photovoltaic thermal air collector

The photovoltaic thermal air collector (PVTAC) was constructed with a polycrystalline PV module, glass cover, wavy-shaped absorber plate, plain base plate, galvanized iron sheet, and insulation material. The dimension of the

Fig. 1 a Schematic view of the PVT solar dryer; **b** cross-sectional view of PVT air collector
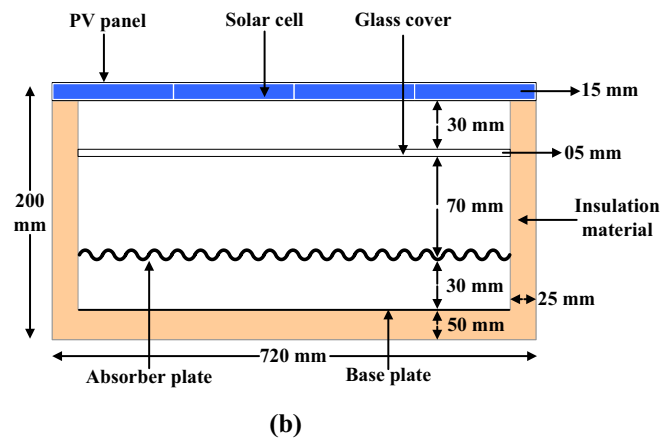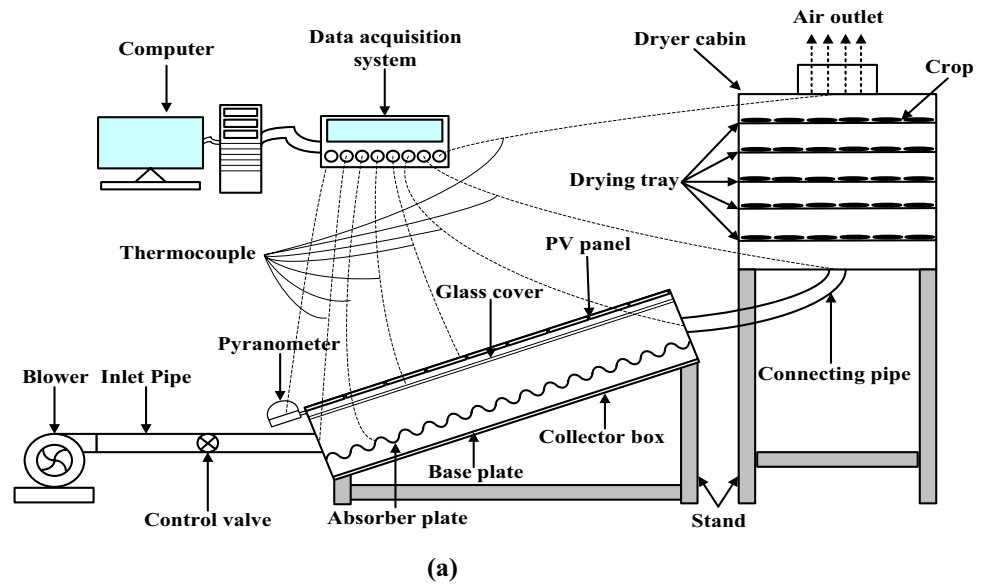

(a)

(b)

Table 1 Specification and material used of various components for PVT solar dryer

Components	Materials	Measurements
Photovoltaic thermal air collector (PVTAC)	G.I. sheet	1.10 m × 0.72 m × 0.20 m (*l* × *w* × *h*)
Dryer cabin	Mild steel sheet	0.47 m × 0.47 m × 0.96 m (*l* × *w* × *h*)
Drying tray	Wood and aluminum mesh	0.40 m × 0.40 m (l × w)
Glass cover	Transparent glass	1.06 m × 0.67 m × 0.005 m (*l* × *w* × *h*)
PV module	Polycrystalline	1.06 m × 0.67 m × 0.015 m (*l* × *w* × *h*)
Absorber plate	G. I. sheet	0.001 m (t)
Base plate	G. I. sheet	0.001 m (t)
Insulation	Polyurethane foam	0.025 and 0.050 m (t)
Inlet and outlet pipe	P.V.C	0.05 m (d)

PVTAC was 1.10 m × 0.72 m × 0.20 m. The PVTAC was oriented in the south direction with an inclination of 24.83°. The PV panel (100 Wp) was used in PVTAC to run the blower and to transfer thermal energy for drying purposes.

The PV module dimension was 1.06 m × 0.67 m × 0.015 m. The glass cover (0.005 m thickness) was used as a glazing layer, 0.03 m below the PV module. A wavy shape absorber plate with a selective coated black paint and thickness of

0.001 m was used to collect the thermal energy. The base plate was placed at the bottom of the PVTAC, 0.03 m below the absorber plate. Polyurethane foam was used as an insulating material having a thickness of 0.05 m and 0.025 m. The cross-sectional view of the PVTAC is illustrated in Fig. 1b. The circulation of ambient air into the PVT air collector was done with the help of a blower with a capacity of 40 Wp. A control valve was attached to regulate the air mass flow rate.

Dryer cabin

The dryer cabin with dimensions of 0.47 m×0.47 m×0.96 m was fabricated with MS sheet. The drying cabin included 05 drying trays. The dimension of each tray was 0.40 m×0.40 m and made of wooden material and aluminum mesh. All sides of the dryer cabin were insulated with 0.05 m of polyurethane foam, and a door was provided to allow loading/unloading of the product. A space of 0.016 m was given between the drying trays to maintain the equilibrium moisture removal. The moisture of the product was removed by blowing and extracting hot air through the lower and upper end of the dryer cabin, respectively.

Experimental procedure

The experiments were carried out from September 18 to 20, 2019, at NIT Silchar, Assam, India, over an 8-h period during a day (8:00 h to 16:00 h). The tomato was selected as a drying crop due to its high moisture content and easy availability. For uniform moisture, tomatoes were cut into thin slices with a thickness of 0.005 m. Total 5 kgs of tomatoes were used for drying within the PVT solar dryer, and each drying tray contained 1 kg of tomatoes. For comparison of the drying sample in PVTSD and OSD, 200 gms of tomato samples were placed in outdoor conditions. The weight of the sample was measured at a time interval of 15 min. The experimental procedures were continued until the samples reached their targeted moisture level. The product samples were stored after the daily experiment, and in the next day, the drying experiment was started with these samples. Drying trays were interchanged every 30 min for removing equal moisture of the product in the dryer cabin.

Instrumentation

The global solar radiation was recorded using a pyranometer (Kipp & Zonen-CMP6). The RTD (PT-100)-type temperature sensor was used to measure the temperature readings at different positions of the experimental setup. Ambient air, dryer inlet air, and dryer outlet air relative humidity were recorded by a thermo-hygrometer (Testo-605i). The air velocity in the different positions of the experimental setup was measured using a hot wire anemometer (Testo-405i). The digital balance (Wensar-TTB3) was used to check the product weight at every 15 min interval. The data collected by the various instruments were recorded in the data acquisition system (DataTaker-DT85). Table 2 summarizes the measured parameters and instrument specifications recorded by the various instruments during the experiments.

Experimental uncertainty

Uncertainty and error can arise in the experimental procedure from measurements of various parameters (Das et al. 2020). The uncertainty calculation of the various parameters measured in the experimental procedure is given in Table 3.

$$U_R = \left[\left(\frac{\partial R}{\partial Z_1} U_1 \right)^2 + \left(\frac{\partial R}{\partial Z_2} U_2 \right)^2 + \cdots + \left(\frac{\partial R}{\partial Z_n} U_n \right)^2 \right]^{\frac{1}{2}}$$

(1)

where U_R is the total uncertainty, U_1, U_2, …, U_n are independent uncertainties, and Z_1, Z_2, …, Z_n are independent variables.

Performance evaluation

An energy and exergy analysis was carried out to indicate the useful energy achieved and estimate the losses in the system. The drying analysis was carried out to evaluate the moisture parameters and drying rate of the sample. Drying models were compared using statistical analysis. To perform the energy balance, the following assumptions were made:

Table 2 Measured parameters and instrument specifications

Instrument name and model	Measuring parameter	Range	Accuracy
Pyranometer (Kipp & Zonen CMP6)	Solar radiation	0–2000 W/m^2	±1%
Data acquisition system (DataTaker DT85)	Data collection	–	±0.01%
Thermo-hygrometer (Testo 605i)	Relative humidity	0–100% RH	±3%
Hot wire anemometer (Testo 405i)	Air velocity	0–30 m/s	±0.2%
Digital balance (Wensar TTB3)	Weight	0–3 kg	±0.1%
RTD (PT-100)	Temperature	−200 to 600 °C	±0.2%

Table 3 Uncertainty calculation for various parameters

Parameters	Uncertainty calculation	Uncertainty value
Solar radiation	$W_{SR} = \left[(W_{pyranometer}) + (W_{reading})\right]^{\frac{1}{2}}$	$W_{SR} = \left[(1)^2 + (1)^2\right]^{\frac{1}{2}} = 1.41$
Temperature	$W_T = \left[(W_{RTD})^2 + (W_{connection\ point})^2 + (W_{reading})^2\right]^{\frac{1}{2}}$	$W_T = \left[(.0.1)^2 + (0.1)^2 + (0.1)^2\right]^{\frac{1}{2}} = 0.17$
Relative humidity	$W_{RH} = \left[(W_{thermo\text{-}hygrometer})^2 + (W_{reading})^2\right]^{\frac{1}{2}}$	$W_{RH} = \left[(0.1)^2 + (0.1)^2\right]^{\frac{1}{2}} = 0.14$
Air velocity	$W_{AV} = \left[(W_{hot\ wire\ anemometer})^2 + (W_{reading})^2\right]^{\frac{1}{2}}$	$W_{AV} = \left[(0.1)^2 + (0.1)^2\right]^{\frac{1}{2}} = 0.14$
Moisture loss	$W_{ML} = \left[(W_{digital\ balance})^2 + (W_{reading})^2\right]^{\frac{1}{2}}$	$W_{ML} = \left[(0.01)^2 + (0.01)^2\right]^{\frac{1}{2}} = 0.014$
Total uncertainty	$W_{TOTAL} = \left[(W_{SR})^2 + (W_T)^2 + (W_{RH})^2 + (W_{AV})^2 + (W_{ML})^2\right]^{\frac{1}{2}}$	$W_{TOTAL} = \left[(1.41)^2 + (0.17)^2 + (0.14)^2 + (0.14)^2 + (0.014)^2\right]^{\frac{1}{2}} = \pm1.43$

- The heat transfer process is one-dimensional and steady state
- Specific heat of air is constant.
- Thermal properties of air remain unchanged during the entire process.
- Thermal losses are neglected.

Energy modeling

The thermal efficiency of PVTAC (η_{PVTAC}) was calculated by dividing the net amount of heat generated (Q_g) by the PVTAC by the total energy available (Q_{av}) on the PVTAC surface (Debnath et al. 2018):

$$\eta_{PVTAC} = \frac{Q_g}{Q_{av}} \tag{2}$$

Mass flow rate and difference in temperature of working fluid affect the heat generation.

The heat generated by the PVTAC was evaluated as (Debnath et al. 2018):

$$Q_g = m_{wf}\, c_{pwf}\left(T_{co} - T_{ci}\right) \tag{3}$$

where m_{wf} is working fluid mass flow rate, c_{pwf} is working fluid specific heat, and T_{co} and T_{ci} are collector outlet and inlet air temperature, respectively.

The amount of energy available mainly depends on solar radiation intensity. The total energy available on the surface of the PVTAC is estimated as (Debnath et al. 2018):

$$Q_{av} = A_m I(s) \tag{4}$$

where $I(s)$ is solar radiation intensity and A_m is module area.

The PVT dryer efficiency (η_{PVTD}) is described as the fraction of the heat utilized for evaporation of sample moisture (Q_e) to the heat available for evaporation (Q_{av}) in the PVT dryer. The blower consumption is not considered for the calculation of PVT dryer efficiency due to the use of a self-driven blower (Vijayan et al. 2016).

$$\eta_{PVTD} = \frac{Q_e}{Q_{av}} \tag{5}$$

The heat required to evaporate the sample moisture is expressed as (Vijayan et al. 2016):

$$Q_e = m_e h_v \tag{6}$$

where m_e is mass of evaporation and h_v is the latent heat of vaporization.

Heat utilization factor (*HUF*) is the proportion of the heat used in the dryer cabin to the heat obtained in the collector box. Heat utilization factor is expressed as (Prakash et al. 2016):

$$HUF = \frac{T_{dci} - T_{dco}}{T_{co} - T_{ci}} \tag{7}$$

where T_{dco} and T_{dci} are dryer cabin inlet and outlet temperature, respectively.

The coefficient of performance (COP) is the proportion of the total heat used in the system to the total heat obtained by the system. The coefficient of performance is expressed as (Prakash et al. 2016):

$$COP = \frac{\left(T_{dco} - T_{dci}\right) + \left(T_{co} - T_{ci}\right)}{\left(T_{co} - T_{ci}\right)} \tag{8}$$

The relation between HUF and COP is described as:

$$HUF + COP = 1 \tag{9}$$

Drying effectiveness (DE) is the proportion of the relative humidity of the dryer cabin outlet to the relative humidity of the dryer cabin inlet. Drying effectiveness is expressed as (Prakash et al. 2016):

$$DE = \frac{\gamma_{dco}}{\gamma_{dci}} \tag{10}$$

where γ_{dco} and γ_{dci} are the relative humidity at the dryer cabin outlet and inlet, respectively.

The collector efficiency factor ($\Delta T/I$) is the proportion of the temperature difference of PVT air collector box to the available solar radiation. The collector efficiency factor is expressed as (Das et al. 2020):

$$\Delta T/I = \frac{T_{co} - T_{ci}}{I(s)} \tag{11}$$

The electrical performance of PVTAC is also measured. The solar cell or PV module electrical efficiency (η_{sc}) is calculated as (Jha et al. 2020b):

$$\eta_{sc} = \eta_{stc}\left[1 - \beta_0\left(T_{sc} - T_0\right)\right] \tag{12}$$

where η_{stc} is standard solar cell efficiency, β_0 is standard efficiency factor, T_0 is standard test temperature of the solar cell, and T_{sc} is solar cell temperature.

Electrical energy (E_{el}) produced by the PV module is evaluated as (Jha et al. 2020b):

$$E_{el} = \tau_g \beta_c \eta_{sc} A_m I(s) \tag{13}$$

where β_c is the packing factor of PV panel, and τ_g is the transmissivity of glass.

The overall energy collected by the PVTAC (Q_{ov}) is the collection of thermal energy and conversion of electrical energy into thermal energy, which is calculated as (Jha et al. 2020b):

$$Q_{ov} = Q_g + \frac{E_{el}}{0.38} \tag{14}$$

where 0.38 is taken as a conversion factor for changing the energy theoretically from electrical to thermal and vice versa (Jha et al. 2020b).

The overall efficiency of PVTAC (η_{ov}) is calculated evaluated by adding electrical and thermal efficiency (Jha et al. 2020b):

$$\eta_{ov} = \eta_{PVTAC} + \frac{\eta_{sc}}{0.38} \tag{15}$$

where the electrical efficiency is converted into thermal efficiency by using an efficiency conversion factor value of 0.38 (Jha et al. 2020b).

Exergy modeling

The second law of thermodynamics describes the phenomenon of exergy analysis. The system achieves the quality of the work in the reversible process. The exergy loss, exergy inflow, and exergy outflow obtained from the process are explained by Eq. (16) (Nazri et al. 2019).

$$\sum Q_{PVTAC,ex,loss} = \sum Q_{PVTAC,ex,in} - \sum Q_{PVTAC,ex,ov} \tag{16}$$

where $Q_{PVTAC,ex,loss}$ is the exergy loss from the PVTAC, $Q_{PVTAC,ex,in}$ is the input exergy to the PVTAC, and $Q_{PVTAC,ex,ov}$ is the overall exergy output obtained from the PVTAC.

The thermal exergy of the PVTAC ($Q_{PVTAC,ex,th}$) is expressed as (Nazri et al. 2019):

$$Q_{PVTAC,ex,th} = m_{wf}\, c_{pwf}\left(T_{co} - T_{ci}\right) \\ - m_{wf}\, c_{pwf}\left(T_a + 273\right) \ln\left(\frac{T_{co} + 273}{T_{ci} + 273}\right) \tag{17}$$

where $Q_{PVTAC,ex,th}$ is the thermal exergy obtained from the PVTAC.

The overall exergy output ($Q_{PVTAC,ex,ov}$) is the sum of electrical and thermal exergy and expressed as (Nazri et al. 2019):

$$Q_{PVTAC,ex,ov} = Q_{PVTAC,ex,th} + E_{el} \tag{18}$$

The exergy input to the PVTAC ($Q_{PVTAC,ex,in}$) is calculated as (Nazri et al. 2019):

$$Q_{PVTAC,ex,in} \\ = A_m I(s)\left[1 - \left(\left(\frac{4}{3}\left(\frac{T_a + 273}{T_s}\right)\right) + \left(\frac{1}{3}\left(\frac{T_a + 273}{T_s}\right)^4\right)\right)\right] \tag{19}$$

where T_s and T_a are the temperature of the sun and ambient, respectively.

The exergy efficiency of the PVTAC ($\eta_{PVTAC,ex}$) is the fraction of thermal exergy to the input exergy, which is calculated as (Nazri et al. 2019):

$$\eta_{PVTAC,ex} = \frac{Q_{PVTAC,ex,th}}{Q_{ex,in}} \tag{20}$$

The overall exergy efficiency of the PVTAC ($\eta_{ov,ex}$) is the sum of the exergy and solar cell or electrical efficiency, which is calculated as (Nazri et al. 2019):

$$\eta_{ov,ex} = \eta_{PVTAC,ex} + \eta_{sc} \tag{21}$$

Drying evaluation parameters

The moisture content is calculated to describe the product drying behavior at different stages of the experiment. The final product dried mass is achieved from the hot air oven method. The moisture content on a dry basis (MC_d) can be evaluated by Eq. (22) (Elkhadraoui et al. 2015):

$$MC_d = \frac{m_o - m_d}{m_d} \tag{22}$$

where m_o and m_d are the product (original and dried) mass, respectively.

The drying rate (DR) can be expressed as (Elkhadraoui et al. 2015):

$$DR = \frac{MC_{t+dt} - MC_t}{dt} = \frac{dM}{dt} \tag{23}$$

where MC_{t+dt} and MC_t are moisture content at time $t+dt$ and time t, respectively.

The moisture ratio (MR) signifies the crop moisture level. It can be determined by Elkhadraoui et al. (2015):

$$MR = \frac{M_t - M_e}{M_i - M_e} \tag{24}$$

where M_i is initial moisture content, M_t is moisture content at time t, and M_e is moisture content at equilibrium stage.

The model values of the predicted moisture ratio (MR_p) are compared to the experimental moisture ratio (MR_e). The proposed (Gupta et al. 2020) drying models for the prediction of moisture ratio are given in Table 4. All models are calculated for OSD and PVTSD. The comparison of various models of drying is based on the values of coefficient of determination (R^2), Chi-square (χ^2), and root mean square error (RMSE), expressed as in Eqs. (25)–(27) (Kouhila et al. 2020):

$$R^2 = 1 - \frac{\sum_{i=1}^{Z} \left(MR_{p,i} - MR_{e,i}\right)^2}{\sum_{i=1}^{Z} \left(\overline{MR_p} - MR_{e,i}\right)^2} \tag{25}$$

$$\chi^2 = 1 - \frac{\sum_{i=1}^{Z} \left(MR_{p,i} - MR_{e,i}\right)^2}{Z - z} \tag{26}$$

$$RMSE = \sqrt{\frac{1}{Z} \sum_{i=1}^{Z} \left(MR_{p,i} - MR_{e,i}\right)^2} \tag{27}$$

where $MR_{p,i}$ and $MR_{e,i}$ are predicted and experimental moisture ratio, respectively, and Z and z are total observations and constants in the model.

Environ-economic evaluation parameters

The environmental impact and economic viability of this system are determined by calculating the following parameters:

Embodied energy

Embodied energy defines the energy needed to manufacture any part of the system. The embodied energy assessment is carried out to identify the total energy consumed by the materials to develop the system (Saini et al. 2017).

CO_2 emission

The CO_2 emission describes embodied energy consumption in manufacturing all parts of the system in proportion to the system life. An extent of 0.98 is the average value of CO_2 emission in kg for generating the electricity per kWh from coal (Saini et al. 2017).

$$CO_2 \text{ emission per year} = \frac{E_i}{L_s} \times 0.98 \text{ kg} \tag{28}$$

where E_i is embodied energy and L_s is system life.

CO_2 mitigation

$$\text{Total } CO_2 \text{ mitigation throughout the system life} = E_o \times L_s \times Z \tag{29}$$

where E_o is annual energy output by the system and Z is CO_2 mitigation in kg per unit kWh.

$$\text{Total } CO_2 \text{ emission by the system} = E_i \times Z \tag{30}$$

and

$$Z = \frac{1}{1 - L_{al}} \times \frac{1}{1 - L_{tl}} \times 0.98 \text{ kg/kWh} \tag{31}$$

where L_{al} is appliances losses, and L_{tl} is transmission losses.

The net CO_2 mitigation by the system is calculated by Saini et al. (2017):

$$CO_2 \text{ mitigation} = \left(E_o \times L_s - E_i\right) \times Z \text{ kg} \tag{32}$$

Carbon credit earned

The earning (carbon credit) from the experimental setup is evaluated accordingly international standard of CO_2 mitigation traded at 10 \$ per ton (Saini et al. 2017):

$$\text{Carbon credit earned} = CO_2 \text{ mitigation} \times 10 \text{ US(\$)} \tag{33}$$

Energy payback time (EPBT)

The time taken by the system for payback is the equivalent energy in comparison with the energy consumed for manufacturing the experimental setup. The energy payback time is expressed as (Saini et al. 2017):

Table 4 Calculated drying model constants, statistical parameters of proposed and established drying models (Gupta et al. 2020) for OSD and PVTSD

Drying model	Model equation	Drying model constants		Statistical parameters	
		OSD	PVTSD	OSD	PVTSD
Newton	$MR = e^{(-kt)}$	$k = 0.029581196$	$k = 0.045521497$	$R^2 = 0.99381, \chi^2 = 4.19448E\text{-}4, RMSE = 0.02048, Adj. R^2 = 0.99374$	$R^2 = 0.98896, \chi^2 = 7.62149E\text{-}4, RMSE = 0.02761, Adj. R^2 = 0.98874$
Page	$MR = e^{(-kt^n)}$	$k = 0.009643781, n = 1.308066353$	$k = 0.011851156, n = 1.422265052$	$R^2 = 0.99888, \chi^2 = 1.01572E\text{-}4, RMSE = 0.01008, Adj. R^2 = 0.99886$	$R^2 = 0.99949, \chi^2 = 5.09778E\text{-}5, RMSE = 0.00714, Adj. R^2 = 0.99948$
Modified Page	$MR = e^{(-(kt)^n)}$	$k = 0.029581196, n = 1$	$k = 0.045521497, n = 1$	$R^2 = 0.99381, \chi^2 = 4.19448E\text{-}4, RMSE = 0.02048, Adj. R^2 = 0.99374$	$R^2 = 0.98896, \chi^2 = 7.62149E\text{-}4, RMSE = 0.02761, Adj. R^2 = 0.98874$
Henderson and Pabis	$MR = a\, e^{(-kt)}$	$k = 0.032582026, a = 1.101278958$	$k = 0.05100606, a = 1.120932138$	$R^2 = 0.98902, \chi^2 = 9.22317E\text{-}4, RMSE = 0.03037, Adj. R^2 = 0.98889$	$R^2 = 0.98204, \chi^2 = 0.00161, RMSE = 0.04008, Adj. R^2 = 0.98170$
Modified Henderson and Pabis	$MR = a\, e^{(-kt)} + b\, e^{(-gt)} + c\, e^{(-ht)}$	$k = -0.009847678, a = -0.03277925, b = 1.211906511, c = -0.184188403, g = 0.030547494, h = 0.157210138$	$k = 0.014373024, a = 1.606882912, b = -0.214658127, c = -0.230489271, g = -0.041231883, h = -0.039529082$	$R^2 = 0.99973, \chi^2 = 2.44152E\text{-}5, RMSE = 0.00494, Adj. R^2 = 0.99973$	$R^2 = 0.99901, \chi^2 = 9.8386E\text{-}5, RMSE = 0.00992, Adj. R^2 = 0.99900$
Two-term	$MR = a\, e^{(-k_0 t)} + b\, e^{(-k_1 t)}$	$k_0 = 0.041372112, k_1 = 0.090943307, a = 1.64515551, b = -0.655819888$	$k_0 = 0.080988349, k_1 = 0.061714863, a = 3.003680939, b = -1.113950974$	$R^2 = 0.99820, \chi^2 = 1.59315E\text{-}4, RMSE = 0.01262, Adj. R^2 = 0.99817$	$R^2 = 0.99930, \chi^2 = 6.84861E\text{-}5, RMSE = 0.00828, Adj. R^2 = 0.99928$
Logarithmic	$MR = a\, e^{(-kt)} + c$	$k = 0.023027993, a = 1.217539938, c = -0.167986064$	$k = 0.051006091, a = 1.21753299, c = -0.082666616$	$R^2 = 0.99830, \chi^2 = 1.54825E\text{-}4, RMSE = 0.01244, Adj. R^2 = 0.99828$	$R^2 = 0.98204, \chi^2 = 0.00161, RMSE = 0.04008, Adj. R^2 = 0.98170$
Wang and Singh	$MR = 1 + a\, t + b\, t^2$	$a = -0.022038745, b = 0.000124653$	$a = -0.033247878, b = 0.000273655$	$R^2 = 0.99877, \chi^2 = 1.08035E\text{-}4, RMSE = 0.01039, Adj. R^2 = 0.99875$	$R^2 = 0.99739, \chi^2 = 2.40618E\text{-}4, RMSE = 0.01551, Adj. R^2 = 0.99734$
Two-term exponential	$MR = a\, e^{(-kt)} + (1-a)\, e^{(-kat)}$	$a = 1.861609139, k = 0.043092843$	$a = 1.955138818, k = 0.069830788$	$R^2 = 0.99828, \chi^2 = 1.53341E\text{-}4, RMSE = 0.01238, Adj. R^2 = 0.99826$	$R^2 = 0.99812, \chi^2 = 1.83161E\text{-}4, RMSE = 0.01353, Adj. R^2 = 0.99808$
Verma et al	$MR = a\, e^{(-kt)} + (1-a)\, e^{(-gt)}$	$k = -0.001530751, a = -1.011326149, g = 0.023124429$	$k = 0.121027721, a = -1.454122335, g = 0.038166935$	$R^2 = 0.99649, \chi^2 = 2.97766E\text{-}4, RMSE = 0.01726, Adj. R^2 = 0.99645$	$R^2 = 0.99839, \chi^2 = 1.57797E\text{-}4, RMSE = 0.01256, Adj. R^2 = 0.99836$
Diffusion approach	$MR = a\, e^{(-kt)} + (1-a)\, e^{(-kbt)}$	$a = 0.828294109, k = 0.027365759, b = -0.12359954$	$a = -1.688269303, k = 0.1147823, b = 0.658807038$	$R^2 = 0.99485, \chi^2 = 4.40714E\text{-}4, RMSE = 0.02099, Adj. R^2 = 0.99478$	$R^2 = 0.99853, \chi^2 = 1.42783E\text{-}4, RMSE = 0.01195, Adj. R^2 = 0.99850$
Midilli–Kucuk	$MR = a\, e^{(-kt^n)} + b\, t$	$a = 1.004957028, k = 0.012407596, b = -0.000505558, n = 1.219775754$	$a = 0.993785599, k = 0.012701457, b = -0.000502935, n = 1.383208274$	$R^2 = 0.99966, \chi^2 = 3.07157E\text{-}5, RMSE = 0.00554, Adj. R^2 = 0.99966$	$R^2 = 0.99990, \chi^2 = 9.71098E\text{-}6, RMSE = 0.00312, Adj. R^2 = 0.99990$

Table 4 (continued)

Drying model	Model equation	Drying model constants		Statistical parameters	
		OSD	PVTSD	OSD	PVTSD
Proposed model	$MR = a \times e^{(-kt^n)} + b \times e^{(-gt^n)} + c \times e^{(-ht^n)}$	$k=0.0065444$, $a=-0.283670085$, $b=1.375290534$, $c=-0.098447358$, $g=0.02117463$, $h=0.208287206$, $n=1.038110022$	$k=-0.019852305$, $a=-0.004230685$, $b=1.513911848$, $c=-0.513081477$, $g=0.034356254$, $h=0.069658793$, $n=1.161230594$	$R^2=0.99977$, $\chi^2=2.05474\text{E-}5$, RMSE$=0.00453$, Adj. $R^2=0.99977$	$R^2=0.99998$, $\chi^2=6.08529\text{E-}6$, RMSE$=0.00270$, Adj. $R^2=0.99997$

$$\text{EPBT} = \frac{E_i}{E_o} \tag{34}$$

Quality analysis

The color indices, total phenolic content, and total flavonoid content are evaluated to analyze the quality of the dried product.

Evaluation of color indices

Color indices are the most significant parameters for the evaluation of the quality analysis of the drying samples. The values of L^*, a^*, and b^* define the product's color change. The color indices values should be closer to the original values of the fresh product to obtain a better quality of the dried product. The color changed in the product (ΔE) is obtained using Eq. (35) (Lakshmi et al. 2018).

$$\Delta E = \sqrt{\Delta L^{*2} + \Delta a^{*2} + \Delta b^{*2}} \tag{35}$$

where L^* represents lightness in color, a^* denotes a color change from red to green, and b^* represents a change in color from yellow to blue.

Evaluation of total phenolic content

The Folin–Ciocalteu process has been implemented to found the total phenolic content in the drying samples (Lakshmi et al. 2018). The quantity of 0.1 ml Folin–Ciocalteu solution mixed with the 0.1 ml of aliquot. After three-minute reaction, 0.3 ml of 2% sodium carbonate (Na_2CO_3) has been mixed with the solution. The solution is placed under dark light for 2 h to obtain the absorbance value in the spectrophotometer at 760 nm. The measured value is presented in mg gallic of acid equivalent/gm of dry sample (mg/gm).

Evaluation of total flavonoid content

Lakshmi et al. (Lakshmi et al. 2018) has been applied to evaluate the total flavonoid content in the drying sample. The drying sample solution of 0.25 ml is taken for mix with the 1.25 ml of distilled water. After 5 min, the solution of 0.075 ml $NaNO_2$ is added with the 0.15 ml $AlCl_3$ solution and mixed with the previous sample. The solution of 2 ml NaOH and 0.6 ml distilled water are added after 6 min. The solution is well mixed, and absorbance is found at 510 nm in the spectrophotometer. The result of total flavonoid content is described in mg quercetin/gm of dry sample (mg/gm).
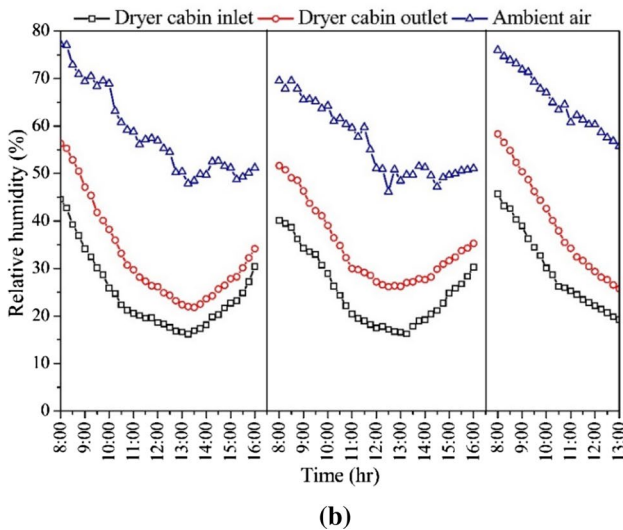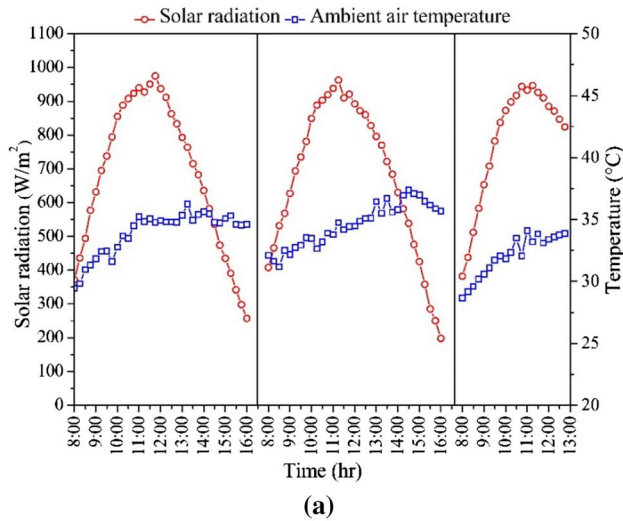
Fig. 2 Variation of **a** solar radiation and ambient air temperature; **b** relative humidity during the test period

Fig. 3 Variation of **a** temperatures of PVT solar dryer; **b** temperature difference of PVT air collector and solar radiation during the test period

Results and discussion

PVT air collector and dryer performance

The experiments were conducted in the month of September under the climatic conditions of North-East India. Figure 2a shows the measured solar radiation and ambient air temperature during test periods. The average solar radiation was 705.00 W/m² and varied from 198.00 to 975.00 W/m². Ambient air temperature values were ranging between 28.65 and 37.39 °C. The peak solar radiation was reached during noon, and the ambient temperature gradually increased over the test period. The relative humidity was also measured to analyze the influence of this parameter on the drying performance. The humidity level of air in the dryer cabin
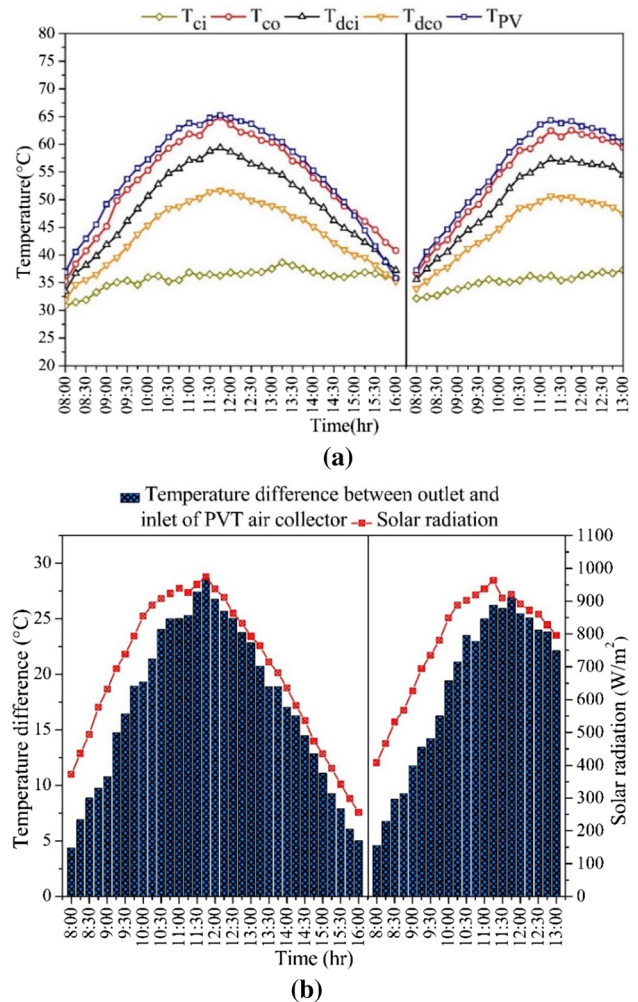
outlet and inlet was lower than ambient conditions. This is a suitable condition for achieving a better drying rate in the PVT solar drying system. Figure 2b shows the measured humidity level at the dryer outlet and inlet and also in the ambient air. The measured ambient air humidity was in the range of 47.88–77.21%. The humidity at the dryer's inlet was between 16.21 and 45.74%, and at the dryer's outlet was 21.83% to 58.32%. This was due to the absorbance of moisture from the crop. In general, a lower humidity level was attained in the dryer cabin by supplying hot air to extract a higher level of moisture from the crop.

Figure 3a represents the temperature of the PV panel (T_{PV}), PVT air collector inlet (T_{ci}) and outlet (T_{co}), and dryer cabin inlet (T_{dci}) and outlet (T_{dco}), respectively, when the air mass flow rate was 0.015 kg/s. The temperature of the PV panel was ranged between 38.50 and 65.24 °C and increased with respect to incident solar radiation on the surface. The

PVT air collector inlet and outlet temperatures were in the range from 30.85 to 38.64 °C and 35.21 °C to 64.91 °C, respectively, and the dryer cabin inlet and outlet temperatures were varied from 33.46 to 59.38 °C and 31.85 °C to 51.64 °C, respectively. Thermal energy collected in the PVT air collector increased the inlet air temperature. The hot air was supplied to the dryer cabin. Temperature reduction between the collector outlet and dryer inlet occurred due to some convection losses in the connecting pipe. The temperature variations within the PVT system depend on the level of solar radiation on the absorber surface. Figure 3b shows the PVT air collector outlet and inlet temperature difference and the solar radiation variation with time. After the start of the experiment, the temperature difference increased rapidly with the changes in solar radiation level and decreased linearly with the reduction in solar radiation level. The maximum temperature difference was recorded as 28.64 °C on the first day and 26.89 °C on the second day of the experiment. The same hot air from the collector was then supplied to the dryer cabin. The average temperature difference between the inlet and outlet of the collector was found to be 17.88 °C. The solar radiation levels affected the temperature ranges of the solar dryer. The heat flow in the dryer cabin was varied by changing the temperature range of the solar dryer. A higher heat transfer is required in the PVT solar dryer to remove faster moisture evaporation from the crop.

Heat utilization factor (HUF) variation and coefficient of performance (COP) variation with time is presented in Fig. 4a. The values of HUF and COP are estimated in the range from 0.24 to 0.39 and 0.61–0.76 on the first day, and the same ranges from 0.24 to 0.36 and 0.64 to 0.76 on the second day of the experiment. Results show that both the parameters are affected by each other as an increase of one parameter decreases the other parameter and vice versa. The higher value of HUF is preferred for drying purposes due to the more heat that may be utilized in the drying cabin. The average value of HUF and COP are achieved as 0.29 and 0.71, respectively. Similar trends of HUF and COP have been observed by Chauhan et al. (2018b), which was in the range of 0.11–0.79 and 0.22–0.88, respectively. Figure 4b shows the variation of PVT solar dryer efficiency (η_{PVTD}), drying effectiveness (DE), and collector efficiency factor ($\Delta T/I$) variation during the test period. Higher dryer efficiency values are obtained on the first day compared to the second day. This may cause more moisture to be present on the crop surface, and thus, more water mass evaporation takes place from the crop in the initial period. The PVT dryer efficiency values are calculated in 40.21–63.13% on the first day and 6.20–53.02% on the second day of the experiment, respectively. The average value of PVT dryer efficiency is found to be 34.98%. The results obtained from this study are compared with various reported studies conducted on similar types of drying systems (indirect mode) with similar
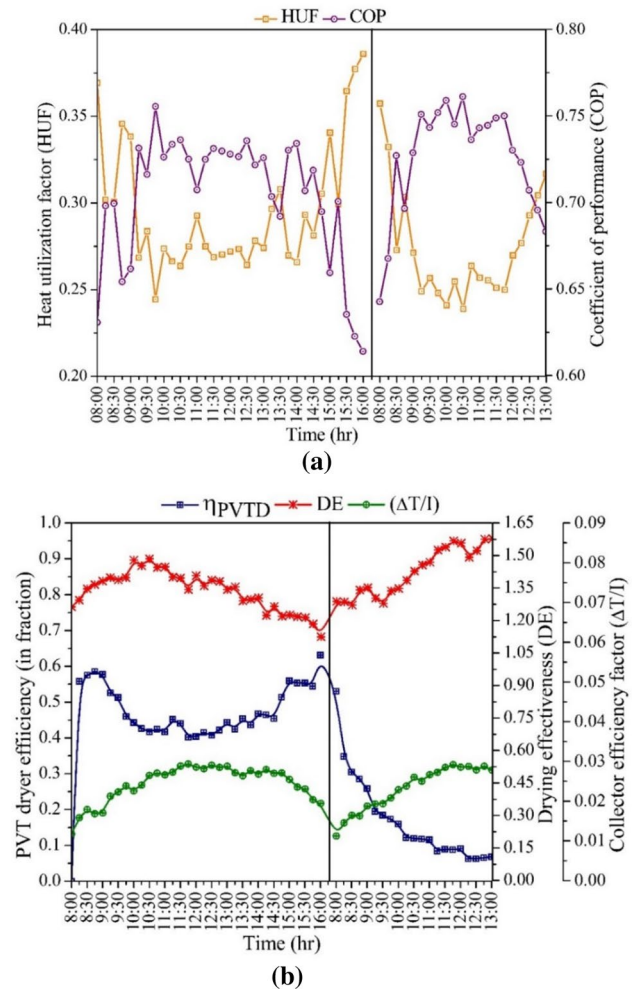

Fig. 4 Variation of **a** HUF and COP; **b** PVT solar dryer efficiency (η_{PVTD}), drying effectiveness (DE), and collector efficiency factor ($\Delta T/I$)

experimental conditions and similar crop types. For example, the dryer efficiency of 12.00% under similar outdoor conditions was reported by Lakshmi et al. (2018); within 8.80–10.66% by Cesar et al. (2020); within 12.92–27.84% by Bhardwaj et al. (2018); within 30.90–33.80% by Wang et al. (2017); and 19.00% by Vijayan et al. (2016). Furthermore, the results indicated a higher dryer efficiency value in PVT solar dryer compared to the conventional dryer used in the earlier studies.

In addition, the drying effectiveness (DE) and PVT collector efficiency factor ($\Delta T/I$) were measured to evaluate the performance of PVT solar dryer. The higher the dehumidification in the dryer cabin, the higher is the drying effectiveness. Maximum drying effectiveness is seen in the afternoon of the day due to the higher solar radiation availability. The drying effectiveness varied from 1.12 to 1.48 and 1.27 to 1.58 on the first and second days. The collector efficiency factor was found to vary within the same range

(0.11 to 0.029) over two test days, indicating that the PVT system adequately utilized the energy for both days. The higher temperature difference is preferable to obtain a higher collector efficiency factor, and it has been achieved in the present study.

PVT solar dryer energy analysis

The energy parameters (electrical, thermal, and overall thermal) are investigated in the PVT solar dryer to evaluate the system's performance. The effect of modification of the PVT air collector in the solar dryer has been tested. It can be seen from Fig. 5a, the PV module temperature varied from 35.82 to 65.24 °C and 37.24 to 64.34 °C, on the first and second days, respectively, and the PV efficiency ranged from 12.28 to 14.27% and 12.34 to 14.17% on the first and second days, respectively. The efficiency of the PV module is inversely proportional to the module temperature. The results obtained in this related to PV efficiency is comparable with other reported study (Tiwari and Tiwari 2017a, 2018).

PVT air collector allows the reduction of heat losses and enhances the energy utilization rate in the system. PVT solar dryer energy gain is presented in Fig. 5b. The energy gain is directly influenced by available solar radiation. The estimated electrical energy (E_{el}) ranged from 20.53 to 67.05 W and 32.37 W to 66.55 W, on the first and second days, respectively, and the thermal energy varied from 65.73 to 431.75 W and 69.19 W to 405.37 W, respectively. The higher thermal energy was achieved at a higher temperature difference. The overall thermal energy (Q_{ov}) was found to be between is estimated in the range from 129.40 to 608.19 W and 154.39 W to 573.02 W, on the first and second days, respectively. The total generation of overall thermal energy, thermal energy, and electrical energy from the PVT solar dryer was 5.48 kWh, 3.64 kWh, and 0.70 kWh. These values are compared with the study conducted by Tiwari and Tiwari (2017a) with values obtained as 3.24 kWh, 2.63 kWh, and 0.23 kWh and by Tiwari and Tiwari (2017b) with corresponding values reported as 1.65 kWh, 0.60 kWh, and 0.40 kWh. More generation of energy by the PVT system is achieved in this study compared to previous studies.

Variation of PVT air collector efficiencies with time is depicted in Fig. 5c. Results indicate that higher ranges are achieved for thermal and overall thermal efficiency compared to electrical efficiency. This is attained with the effective use of available solar radiation and by overcoming the PVT system's losses. The thermal efficiency (η_{PVTAC}) is varied from 24.88 to 62.37% and 23.89 to 61.99% for the first and second days, respectively. The overall thermal efficiency (η_{ov}) is ranged between 62.24 and 94.69 and 61.18 and 94.50% for the first and second days, respectively. The average efficiency of electrical energy output, thermal energy output, and overall thermal energy output is 12.99%,
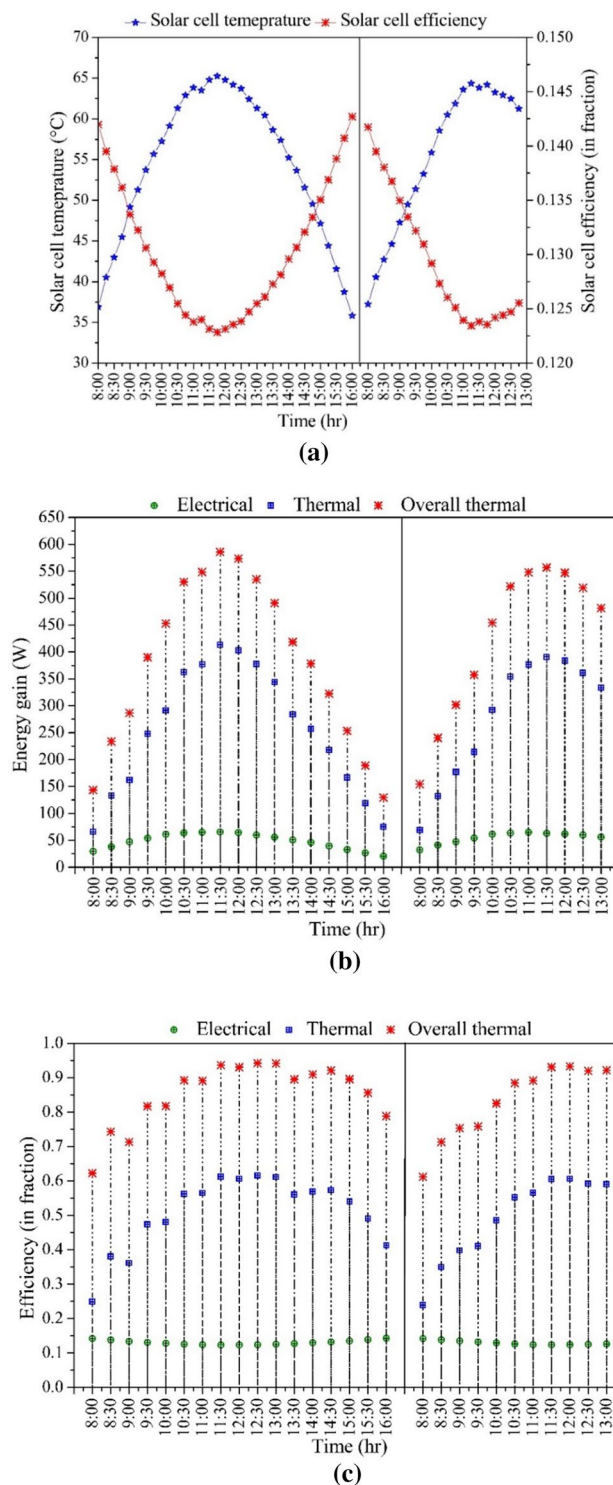

Fig. 5 Variation of PVT air collector **a** solar cell temperature and solar cell efficiency; **b** energy gain; **c** energy efficiency

50.79%, and 84.99%. In the present study, significantly efficient results are obtained compared with the previous study of Tiwari et al. (2018), in which the corresponding efficiency values as 11.26%, 26.68%, and 56.30% were obtained. The

present results are comparable to the previous study performed by Tiwari and Tiwari (2017a), who reported the corresponding efficiency values as 11.80–13.20%, 27.37%, and 61.56%. Similarly, the present results are again in line with the results of Tiwari and Tiwari (2017b), who measured the corresponding efficiency ranges as 12.22–14.21%, 5.84–13.44%, and 39.05–47.04%.

PVT solar dryer exergy analysis

The actual amount of utilization of energy by the PVT solar dryer is examined by using exergy analysis. The exergy gain from the PVT solar dryer is depicted in Fig. 6a. Solar radiation is the main cause of exergy generation. The electrical exergy (E_{el}) was found to be calculated within 20.53 W to 67.05 W and 32.37 W to 66.55 W on the first and second days, respectively, and the thermal exergy ($Q_{PVTAC,ex,th}$) was from 37.51 to 253.30 W and 39.37 W to 237.23 W, respectively. The overall exergy ($Q_{PVTAC,ex,ov}$) ranged from 63.56 W to 320.35 W and 71.75 W to 300.94 W, on the first and second days, respectively. The total overall, thermal, and electrical exergy generation by the PVT solar dryer is 2.82 kWh, 2.12 kWh, and 0.70 kWh, respectively. It is essential to mention that the higher thermal exergy extraction from the PVT solar dryer had accelerated the drying process. Furthermore, the assistance of electrical exergy is attained for operating the D.C. fan in the PVT solar dryer.

The exergy efficiency of the PVT solar dryer is illustrated in Fig. 6b. With the increase in the temperature of the PVT solar dryer, the electrical exergy efficiency decreases, and thermal and overall exergy efficiency increases. The electrical exergy efficiency is changed from 12.28 to 14.27% and 12.34% to 14.17% for the first and second days, respectively, and the thermal exergy efficiency is ranged from 15.23 to 39.27% and 14.58% to 38.94%, respectively. The overall exergy efficiency ranged from 29.42 to 51.56% and 28.75% to 51.29% for the first and second days. The average electrical, thermal, and overall exergy efficiency of the PVT solar dryer is 12.99%, 31.67%, and 44.66%, respectively. These values are comparable with the study conducted by Tiwari and Tiwari (2017b), and the reported values were 11.96%, 17.00%, and 28.96%. The variation of PVT solar dryer exergy is revealed in Fig. 6c.

The deviation between the exergy input and overall exergy output is more at the initial stage, and after that, the deviation is noticed for both days. However, high exergy output and exergy losses are recorded at high solar radiation. This is due to more exergy input received during this time. The average value is calculated as 476.65 W for exergy in, 208.73 W for exergy out, and 267.92 W for exergy loss. Similar trends of exergy have also been observed by Vijayan et al. (2020) and Karthikeyan and Murugavelh (2018).
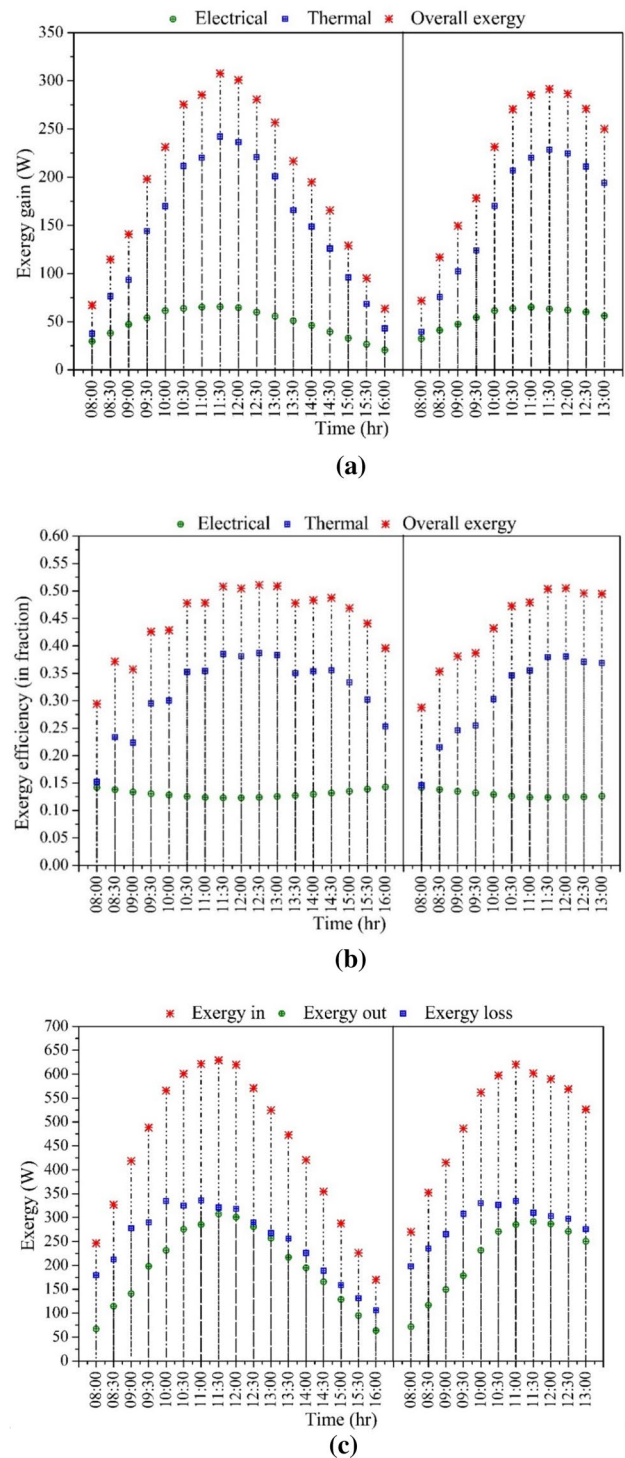
(a)

(b)

(c)

Fig. 6 Variation of **a** exergy gain; **b** exergy efficiency; **c** exergy in, exergy out, and exergy loss in PVT dryer

Drying analysis

Drying is necessary to ensure that the moisture content remains within the acceptable limit for the safe preservation of the crop. Moisture content variations of tomato in

open sun drying (OSD) and PVT solar dryer (PVTSD) are depicted in Fig. 7a. After the drying test, the moisture contents in the samples were reduced from 20.74 (d.b.) to 0.39 (d.b.) in 21 h for OSD and 13 h for PVTSD, indicating that PVTSD is more efficient than OSD process. The reduction of the moisture amount is higher on the first day compared to the second day due to higher moisture presence in the crop on the first day. The drying time of the PVSTD process in this study is better than other reported system studies (26 h for ISD and 17 h for MSD by Cesar et al. 2020).

Variations of moisture ratio for OSD and PVTSD processes are shown in Fig. 7b. It can be seen that the moisture ratio falls rapidly in PVTSD compared to OSD due to the continuous supply of heated air in the dryer cabin, while in the OSD, it depends on the availability of solar radiation and ambient conditions. The moisture ratio of tomatoes is decreased from 1.00 to 0.019 for OSD and PVTSD, respectively. Further, the present results indicate that the drying time is decreased by 38.09% using the proposed efficient PVT solar drying system.

Solar radiation and moisture present in the crop are dominant factors that influence the drying rate. The drying rate of tomatoes for OSD and PVTSD is presented in Fig. 7c. In the initial period of the experiment, a high drying rate is instated for both drying modes due to the crop's higher moisture level. Furthermore, the drying time for PVTSD mode is relatively shorter than the OSD mode due to the increased drying air temperature supplied by PVTSD. The maximum drying rate is calculated at 2.69 (g of water/g of dry matter. hr) and 1.91 (g of water/g of dry matter.hr) for PVTSD and OSD. This proposed PVT solar drying system achieves the improved results of drying rate compared to other reported studies (Samimi-Akhijahani and Arabhosseini 2018, Dorouzi et al. 2018).

Proposed drying model for evaluation of drying kinetics

A new drying model is proposed to predict drying kinetics and drying performance and compared with the previously developed drying models and regression analysis. The best-fitted model was determined with the help of R^2, χ^2, and *RMSE* values. Based on the results obtained, the proposed model has better predicted the moisture ratio than the other drying models for OSD and PVTSD. The statistical results obtained from different drying models are summarized in Table 4 for OSD and PVTSD.

The statistical parameters' values for the proposed model for OSD are calculated as $R^2 = 0.99977$, $\chi^2 = 2.05474\text{E-}5$, RMSE $= 0.00453$, and Adj. $R^2 = 0.99977$. The variance of predicted using the proposed model and experimental moisture ratio for OSD is presented in Fig. 8a.
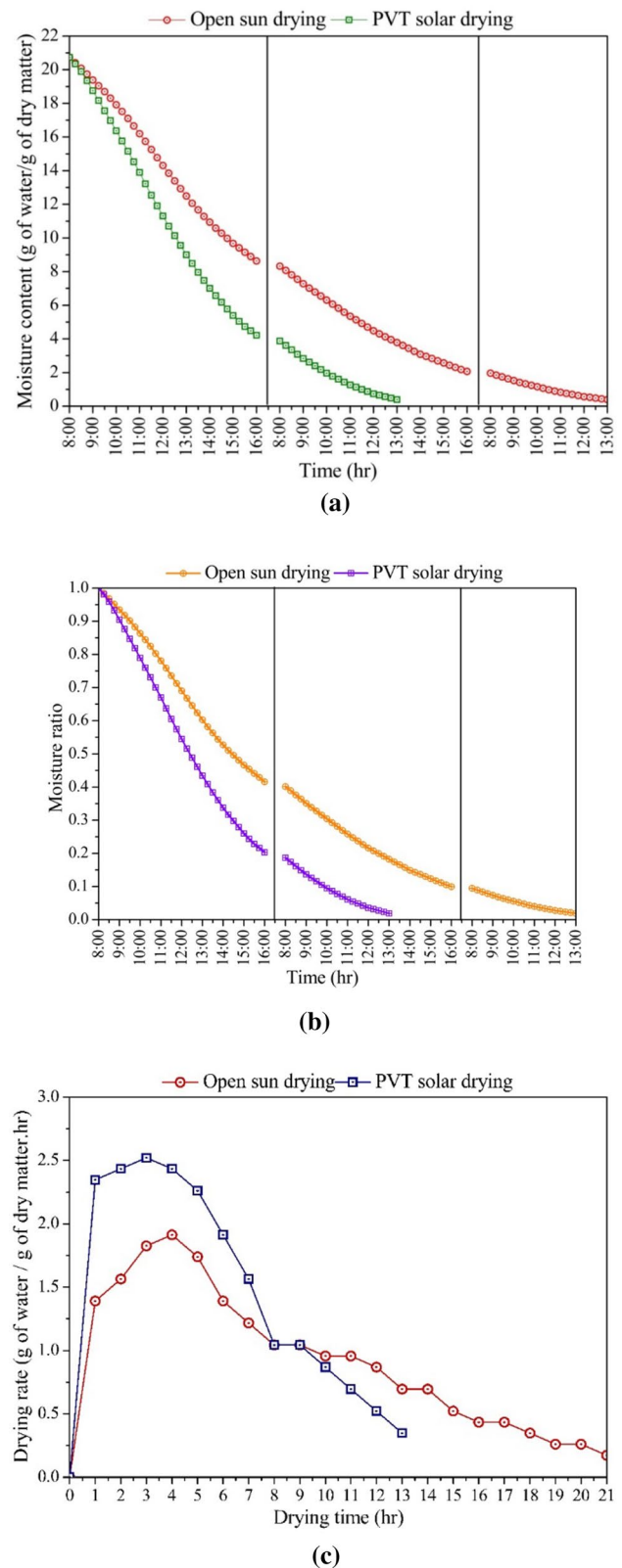
Fig. 7 Variation for OSD and PVTSD processes: **a** moisture content; **b** moisture ratio; **c** drying rate
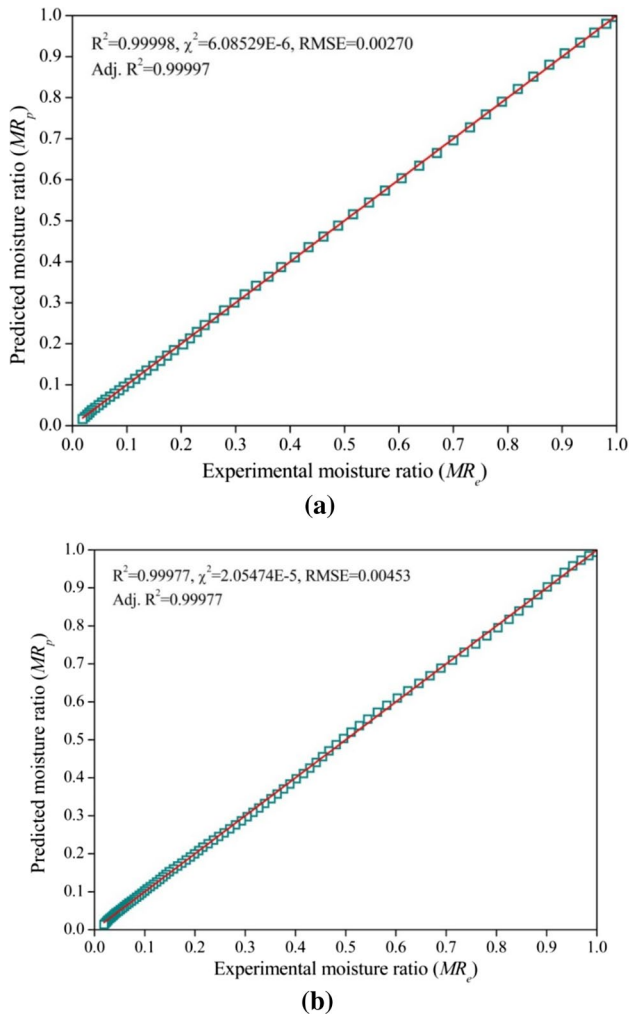
(a)

(b)

Fig. 8 Variation of moisture ratio by the proposed model (predicted and experimental) for **a** OSD, **b** PVTSD

The predicted moisture ratio obtained from the proposed drying model for OSD is calculated as follows.

$$
\begin{aligned}
MR = {}& -0.283670085\, e^{\left(-0.0065444 t^{1.038110022}\right)} \\
& + 1.375290534\, e^{\left(-0.02117463 t^{1.038110022}\right)} \\
& - 0.098447358\, e^{\left(-0.208287206 t^{1.038110022}\right)}
\end{aligned}
\tag{36}
$$

The statistical parameters' values are estimated to be $R^2 = 0.99998$, $\chi^2 = 6.08529E\text{-}6$, RMSE $= 0.00270$, and Adj. $R^2 = 0.99997$ for PVTSD by the proposed model. The variance of predicted using the proposed model and experimental moisture ratio for PVTSD is presented in Fig. 8b.

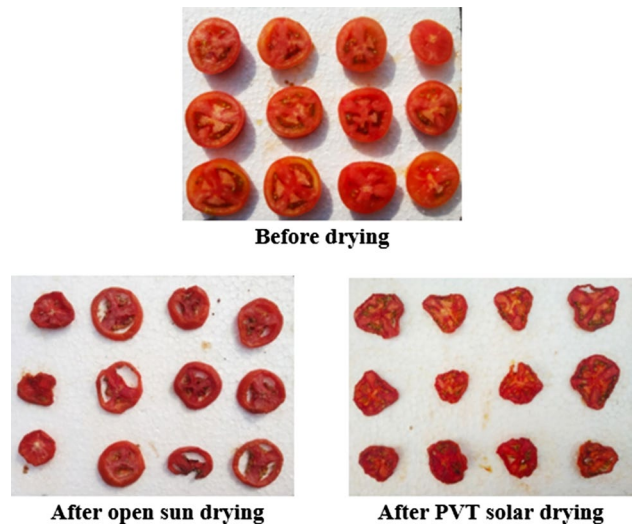The predicted moisture ratio obtained from the proposed drying model for PVTSD is calculated as follows.

Fig. 9 Tomato samples before and after drying

$$
\begin{aligned}
MR = {}& -0.004230685\, e^{\left(0.019852305 t^{1.161230594}\right)} \\
& + 1.513911848\, e^{\left(-0.034356254 t^{1.1611230594}\right)} \\
& - 0.513081477\, e^{\left(-0.069658793 t^{1.161230594}\right)}
\end{aligned}
\tag{37}
$$

The comparisons of sample quality are presented using actual views of tomato before drying, after drying by OSD, and PVTSD in Fig. 9.

Environ-economic analysis

The reliability and sustainability of the system are significantly important for meeting energy demands. Table 5 provides an embodied energy calculation of the components used in the PVT solar dryer. The environmental parameters are estimated for different system life (10 years, 20 years, and 30 years). PVT solar dryer energy payback time is estimated to be 1.45 years. The CO_2 emission of the PVT system decreases to 136.97 kg/y for 10 years, 68.48 kg/y for 20 years, and 45.65 kg/y for 30 years of the system life. At the same time, CO_2 mitigation of the PVT system increases to 18.24 tones for 10 years, 39.58 tones for 20 years, and 60.91 tones for 30 years of the system life. Carbon credit earned by the PVT system is 182.4 $, 395.8 $, and 609.1 $ for 10, 20, and 30 years of the system life. CO_2 emission, CO_2 mitigation, carbon credit earned, and energy payback time (*EPBT*) calculations are shown in Table 6.

Table 5 Embodied energy calculation for various materials used in PVT solar dryer

Sl. no.	Material	Quantity (kg)	Embodied energy (kWh/kg)	Total embodied energy (kWh)
1	Galvanized iron	35.70	8.89	317.37
2	Aluminum	1.20	55.28	71.86
3	Wire mesh steel tray	0.80	9.67	7.74
4	Glass	4.20	7.28	30.58
5	PVC pipe	2.60	19.44	50.54
6	Accessories			
	Handle	0.09	55.28	4.97
	Latch	0.06	55.28	3.32
	Hinge	0.27	55.28	14.92
	Steel screw	0.24	9.67	2.32
7	Solar charge controller	–	–	33.00
8	Battery	–	–	46.00
9	D.C. fan			
	(a) Iron	0.84	8.89	7.47
	(b) Copper wire	0.25	19.61	4.90
10	PV panel	0.71 m^2	1130.60 (kWh/m^2)	802.72
			Total (kWh)	1397.71

Table 6 Estimated environ-economic parameters for PVT solar dryer

Sl. no.	Parameters name	PVT dryer life (Years)		
		10	20	30
1	CO_2 emission (kg/yr)	136.97	68.48	45.65
2	CO_2 mitigation (Tones)	18.24	39.58	60.91
3	Carbon credit earned ($)	182.4	359.8	609.1
4	EPBT (Years)	1.45		

Industrial applications of PVT drying

The drying operations require an enormous amount of energy and modification in the present PVT dryer design leading to cost reduction and improvements in product quality, which will undoubtedly benefit the industries. Many food industries use conventional dryers, which are very expensive, energy-intensive, and unsuitable for a sustainable environment. The PVT drying offers promising solutions in various food processing industries, especially in agricultural crop drying, timber drying, industrial waste drying, dairy industries, and preserving fruits and vegetables. This PVT drying system is suitable for reducing post-harvest losses and increasing farmers' income sources in non-grid-connected areas. The flow chart of the PVT drying process for industrial applications is shown in Fig. 10.

Quality analysis

The quality of tomatoes has been evaluated in PVT solar drying and OSD conditions. The color changes in the
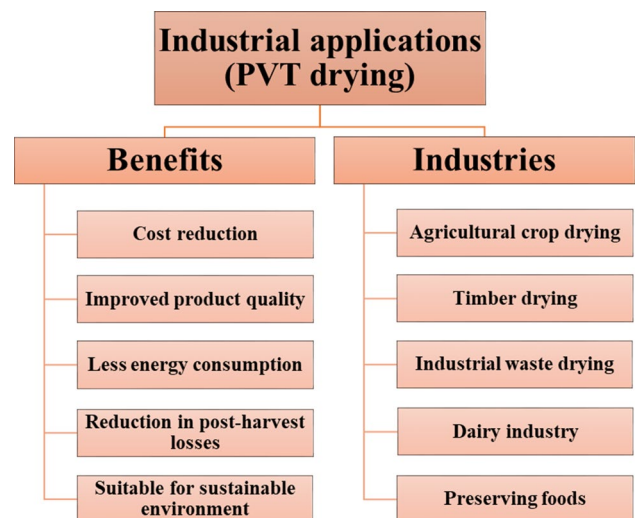

Fig. 10 Industrial applications and benefits of PVT drying

drying samples are defined by measuring color indices. The comparison of color values of tomatoes has been made between the before and after drying. It is revealed that the L^* value decreases, a^* value decreases, and b^* value increases after the drying for tomatoes compared to before drying. The total change in the color indices is evaluated at 5.61 for PVT solar drying and 14.11 for open sun drying. The results indicate that the color change in PVT solar drying is 60.24% less than in the open sun drying. The total phenolic content (mg gallic of acid equivalent/ gm of the dry sample) of tomatoes is determined 271.55, 226.28, and 184.64 before drying, after PVT solar drying,

Table 7 Quality analysis of tomato drying samples

Drying sample	L^*	a^*	b^*	ΔE	Total phenolic content (mg/gm)	Total flavonoid content (mg/gm)
Before drying	41.24	33.75	20.14	–	271.55	218.47
PVT solar drying	38.38	30.47	23.69	31.54	226.28	168.59
Open sun drying	33.54	25.12	28.23	199.21	184.64	147.24

and after open sun drying, respectively. In PVT solar drying, the phenol content remains close to that of the samples before drying. The reduction in phenolic content is measured at 16.67% in PVT solar drying and 32.00% in open sun drying. The total flavonoid content (mg quercetin/gm of the dry sample) of tomatoes is calculated 218.47, 168.59, 147.24 before drying, after PVT solar drying, and after open sun drying, respectively. The decline of the flavonoid content is estimated at 22.83% in PVT solar drying and 32.60% in open sun drying from the original value. The findings of the quality analysis of the tomato drying are seen in Table 7.

Conclusion

This experimental work represents the energetic, exergetic, and environ-economic investigation of newly developed indirect mode solar photovoltaic thermal (PVT) dryer with forced convection for tomato drying, and the following conclusions of this study are drawn:

- The drying time of tomatoes for the proposed system was 61.54% shorter than the OSD process indicating a more efficient drying process compared to the traditional method.
- The proposed mathematical model provided a more accurate predicted moisture ratio than the other drying models for both OSD and PVT solar drying systems.
- The average PVT solar dryer efficiency is 34.98% which is higher than similar types of the system previously developed.
- The average heat utilization factor (HUF) and coefficient of performance (COP) are 0.29 and 0.71, respectively.
- The drying effectiveness (DE) and PVT collector efficiency factor ($\Delta T/I$) are obtained in the range of 1.12–1.58 and 0.011–0.029, respectively.
- This proposed system's electrical, thermal, and overall thermal efficiency are obtained as 12.99%, 50.79%, and 84.99%, respectively.
- Total exergy in, exergy out, and exergy loss of the PVT solar dryer is calculated as 25.74 kWh, 11.27 kWh, and 14.47 kWh, respectively.

- The average thermal and average overall exergy efficiencies of PVT solar dryers are observed to be 31.67% and 44.66% for exergy, respectively.
- The estimated PVT solar dryer energy payback time is 1.45 years.

Conflict of interest The authors hereby confirm that there is no known conflict of interest with the data presented in the present article.

References

Andharia JK, Bhattacharya P, Maiti S (2020) Development and performance analysis of a mixed mode solar thermal dryer for drying of natural rubber sheets in the north-eastern part of India. Sol Energy 208:1091–1102. https://doi.org/10.1016/j.solener.2020.08.051

Bhardwaj AK, Kumar R, Chauhan R (2019) Experimental investigation of the performance of a novel solar dryer for drying medicinal plants in Western Himalayan region. Sol Energy 177:395–407. https://doi.org/10.1016/j.solener.2018.11.007

Chauhan PS, Kumar A, Nuntadusit C, Banout J (2018a) Thermal modeling and drying kinetics of bitter gourd flakes drying in modified greenhouse dryer. Renew Energy 118:799–813. https://doi.org/10.1016/j.renene.2017.11.069

Chauhan PS, Kumar A, Nuntadusit C (2018b) Heat transfer analysis of PV integrated modified greenhouse dryer. Renew Energy 121:53–65. https://doi.org/10.1016/j.renene.2018.01.017

Daghigh R, Shahidian R, Oramipoor H (2020) A multistate investigation of a solar dryer coupled with photovoltaic thermal collector and evacuated tube collector. Sol Energy 199:694–703. https://doi.org/10.1016/j.solener.2020.02.069

Das B, Mondol JD, Debnath S, Pugsley A, Smyth M, Zacharopoulos A (2020) Effect of the absorber surface roughness on the performance of a solar air collector: an experimental investigation. Renew Energy 152:567–578. https://doi.org/10.1016/j.renene.2020.01.056

Debnath S, Das B, Randive PR, Pandey KM (2018) Performance analysis of solar air collector in the climatic condition of North Eastern India. Energy 165:281–298. https://doi.org/10.1016/j.energy.2018.09.038

Dejchanchaiwong R, Arkasuwan A, Kumar A, Tekasakul P (2016) Mathematical modeling and performance investigation of mixed-mode and indirect solar dryers for natural rubber sheet drying. Energy Sustain Dev 34:44–53. https://doi.org/10.1016/j.esd.2016.07.003

Dorouzi M, Mortezapour H, Akhavan HR, Moghaddam AG (2018) Tomato slices drying in a liquid desiccant-assisted solar dryer coupled with a photovoltaic-thermal regeneration system. Sol Energy 162:364–371. https://doi.org/10.1016/j.solener.2018.01.025

Dutta P, Dutta PP, Kalita P (2020) Thermal performance studies for drying of Garcinia pedunculata in a free convection corrugated type of solar dryer. Renew Energy 163:599–612. https://doi.org/10.1016/j.renene.2020.08.118

Elkhadraoui A, Kooli S, Hamdi I, Farhat A (2015) Experimental investigation and economic evaluation of a new mixed- mode solar greenhouse dryer for drying of red pepper and grape. Renew Energy 77:1–8. https://doi.org/10.1016/j.renene.2014.11.090

Erick César LV, Ana Lilia CM, Octavio GV, Isaac PF, Rogelio BO (2020) Thermal performance of a passive, mixed-type solar dryer for tomato slices (Solanum lycopersicum). Renew Energy 147:845–855. https://doi.org/10.1016/j.renene.2019.09.018

Goud M, Reddy MVV, Chandramohan VP, Suresh S (2019) A novel indirect solar dryer with inlet fans powered by solar PV panels: drying kinetics of Capsicum Annum and Abelmoschus esculentus with dryer performance. Sol Energy 194:871–885. https://doi.org/10.1016/j.solener.2019.11.031

Gupta A, Das B, Mondol JD (2020) Experimental and theoretical performance analysis of a hybrid photovoltaic-thermal (PVT) solar air dryer for green chillies. Int J Ambient Energy. https://doi.org/10.1080/01430750.2020.1734658

Hatami S, Payganeh G, Mehrpanahi A (2020) Energy and exergy analysis of an indirect solar dryer based on a dynamic model. J Clean Prod 244:118809. https://doi.org/10.1016/j.jclepro.2019.118809

Jha P, Mondol JD, Das B, Gupta R (2020b) Energy metrics assessment of a photovoltaic thermal air collector (PVTAC): a comparison between flat and wavy collector. Energy Sources Part A Recover Util Environ Eff. https://doi.org/10.1080/15567036.2020.1809563

Jha P, Das B, Gupta R (2019) An experimental study of a photovoltaic thermal air collector (PVTAC): a comparison of a flat and the wavy collector. Appl Therm Eng 163:114344. https://doi.org/10.1016/j.applthermaleng.2019.114344

Jha P, Das B, Gupta R (2020a) Performance of air-based photovoltaic thermal collector with fully and partially covered photovoltaic module. Appl Therm Eng 180:115838. https://doi.org/10.1016/j.applthermaleng.2020.115838

Joshi SS, Dhoble AS (2018) Photovoltaic -thermal systems (PVT): technology review and future trends. Renew Sustain Energy Rev 92:848–882. https://doi.org/10.1016/j.rser.2018.04.067

Karthikeyan AK, Murugavelh S (2018) Thin layer drying kinetics and exergy analysis of turmeric (Curcuma longa) in a mixed mode forced convection solar tunnel dryer. Renew Energy 128:305–312. https://doi.org/10.1016/j.renene.2018.05.061

Kong D, Wang Y, Li M, Keovisar V, Huang M, Yu Q (2020) Experimental study of solar photovoltaic/thermal (PV/T) air collector drying performance. Sol Energy 208:978–989. https://doi.org/10.1016/j.solener.2020.08.067

Kouhila M, Moussaoui H, Lamsyehe H, Tagnamas Z, Bahammou Y, Idlimam A, Lamharrar A (2020) Drying characteristics and kinetics solar drying of Mediterranean mussel (mytilus galloprovincilis) type under forced convection. Renew Energy 147:833–844. https://doi.org/10.1016/j.renene.2019.09.055

Kumar A, Baredar P, Qureshi U (2015) Historical and recent development of photovoltaic thermal (PVT) technologies. Renew Sustain Energy Rev 42:1428–1436. https://doi.org/10.1016/j.rser.2014.11.044

Lakshmi DVN, Muthukumar P, Layek A, Nayak PK (2018) Drying kinetics and quality analysis of black turmeric (Curcuma caesia) drying in a mixed mode forced convection solar dryer integrated with thermal energy storage. Renew Energy 120:23–34. https://doi.org/10.1016/j.renene.2017.12.053

Lamnatou C, Chemisana D (2017) Photovoltaic/thermal (PVT) systems: a review with emphasis on environmental issues. Renew Energy 105:270–287. https://doi.org/10.1016/j.renene.2016.12.009

Nazri NS, Fudholi A, Mustafa W, Yen CH, Mohammad M, Ruslan MH, Sopian K (2019) Exergy and improvement potential of hybrid photovoltaic thermal/thermoelectric (PVT/TE) air collector. Renew Sustain Energy Rev 111:132–144. https://doi.org/10.1016/j.rser.2019.03.024

Prakash O, Kumar A, Laguri V (2016) Performance of modified greenhouse dryer with thermal energy storage. Energy Rep 2:155–162. https://doi.org/10.1016/j.egyr.2016.06.003

Rabha DK, Muthukumar P, Somayaji C (2017) Energy and exergy analyses of the solar drying processes of ghost chilli pepper and ginger. Renew Energy 105:764–773. https://doi.org/10.1016/j.renene.2017.01.007

Saini V, Tiwari S, Tiwari GN (2017) Environ economic analysis of various types of photovoltaic technologies integrated with greenhouse solar drying system. J Clean Prod 156:30–40. https://doi.org/10.1016/j.jclepro.2017.04.044

Samimi-Akhijahani H, Arabhosseini A (2018) Accelerating drying process of tomato slices in a PV-assisted solar dryer using a sun tracking system. Renew Energy 123:428–438. https://doi.org/10.1016/j.renene.2018.02.056

Singh P, Shrivastava V, Kumar A (2018) Recent developments in greenhouse solar drying: A review. Renew Sustain Energy Rev 82:3250–3262. https://doi.org/10.1016/j.rser.2017.10.020

Singh P, Kumar A (2018) Thermal modeling and drying kinetics of gooseberry drying inside north wall insulated greenhouse dryer. Appl Therm Eng 130:587–597. https://doi.org/10.1016/j.applthermaleng.2017.11.028

Tiwari S, Tiwari GN (2016) Exergoeconomic analysis of photovoltaic-thermal (PVT) mixed mode greenhouse solar dryer. Energy 114:155–164. https://doi.org/10.1016/j.energy.2016.07.132

Tiwari S, Tiwari GN (2017a) Energy and exergy analysis of a mixed-mode greenhouse-type solar dryer, integrated with partially covered N-PVT air collector. Energy 128:183–195. https://doi.org/10.1016/j.energy.2017.04.022

Tiwari S, Tiwari GN (2017b) Thermal analysis of photovoltaic thermal integrated greenhouse system (PVTIGS) for heating of slurry in potable biogas plant: an experimental study. Sol Energy 155:203–211. https://doi.org/10.1016/j.solener.2017.06.021

Tiwari S, Tiwari GN, Al-Helal IM (2016) Performance analysis of photovoltaic-thermal (PVT) mixed mode greenhouse solar dryer. Sol Energy 133:421–428. https://doi.org/10.1016/j.solener.2016.04.033

Tiwari S, Agrawal S, Tiwari GN (2018) PVT air collector integrated greenhouse dryers. Renew Sustain Energy Rev 90:142–159. https://doi.org/10.1016/j.rser.2018.03.043

Vijayan S, Arjunan TV, Kumar A (2016) Mathematical modeling and performance analysis of thin layer drying of bitter gourd in sensible storage based indirect solar dryer. Innov Food Sci Emerg Technol 36:59–67. https://doi.org/10.1016/j.ifset.2016.05.014

Vijayan S, Arjunan TV, Kumar A (2020) Exergo-environmental analysis of an indirect forced convection solar dryer for drying bitter gourd slices. Renew Energy 146:2210–2223. https://doi.org/10.1016/j.renene.2019.08.066

Wang W, Li M, Hassanien RHE, Wang Y, Yang L (2018) Thermal performance of indirect forced convection solar dryer and kinetics analysis of mango. Appl Therm Eng 134:310–321. https://doi.org/10.1016/j.applthermaleng.2018.01.115

Authors and Affiliations

A. Gupta[1] · B. Das[1,2] · A. Biswas[1] · J. D. Mondol[2]

✉ B. Das
   bpd@mech.nits.ac.in

[1] PVT Laboratory, Department of Mechanical Engineering,
    National Institute of Technology Silchar, Silchar,
    Assam 788010, India

[2] Centre for Sustainable Technologies, School of the Built
    Environment, Ulster University, Northern Ireland BT37 0QB,
    UK